Vertical profile measurements of lower troposphere ionisation

Article

Published Version

It is advisable to refer to the publisher's version if you intend to cite from the work. See Guidance on citing.
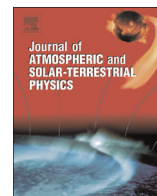
Vertical profile measurements of lower troposphere ionisation

R.G. Harrison [a], K.A. Nicoll [a], K.L. Aplin [b,*]

[a] Department of Meteorology, University of Reading, PO Box 243, Earley Gate, Reading RG6 6BB, United Kingdom
[b] Department of Physics, University of Oxford, Denys Wilkinson Building, Keble Road, Oxford OX1 3RH, United Kingdom

ARTICLE INFO

ABSTRACT

Vertical soundings of the atmospheric ion production rate have been obtained from Geiger counters integrated with conventional meteorological radiosondes. In launches made from Reading (UK) during 2013–2014, the Regener–Pfotzer ionisation maximum was at an altitude equivalent to a pressure of (63.1 ± 2.4) hPa, or, expressed in terms of the local air density, (0.101 ± 0.005) kg m^{-3}. The measured ionisation profiles have been evaluated against the Usoskin–Kovaltsov model and, separately, surface neutron monitor data from Oulu. Model ionisation rates agree well with the observed cosmic ray ionisation below 20 km altitude. Above 10 km, the measured ionisation rates also correlate well with simultaneous neutron monitor data, although, consistently with previous work, measured variability at the ionisation maximum is greater than that found by the neutron monitor. However, in the lower atmosphere (below 5 km altitude), agreement between the measurements and simultaneous neutron monitor data is poor. For studies of transient lower atmosphere phenomena associated with cosmic ray ionisation, this indicates the need for in situ ionisation measurements and improved lower atmosphere parameterisations.

1. Introduction

Molecular cluster ions contribute to the finite electrical conductivity of atmospheric air, permitting current flow in the global atmospheric electric circuit (Rycroft et al., 2000). Cluster ions are formed in the lower troposphere by the ionising effects of natural radioactivity and galactic cosmic rays (GCRs), and, episodically, solar energetic particles (SEPs). Well above the continental surface, GCRs provide the principal source of ionisation. Several possible effects of cluster ions on atmospheric processes are now under active investigation, such as through the electrification of layer clouds associated with current flow in the global circuit (Nicoll and Harrison, 2010), ion-induced nucleation at cloud levels (Kirkby et al., 2011) or radiative absorption by cluster ions (Aplin and Lockwood, 2013). These all require an accurate determination of the spatial and temporal variations in atmospheric ionisation at the relevant altitudes and location.

Ionisation from GCRs can be measured using a number of techniques deployed, variously, at the surface, within the atmosphere or in space. Spacecraft sensors can be used to detect ionising particles, particularly SEPs, but as SEP emissions are sporadic and associated with solar storms, they do not contribute substantially to atmospheric ionisation in normal conditions, and

hence are not considered further. When a primary cosmic ray particle, often a helium nucleus or a proton (Usoskin and Kovaltsov, 2006), enters an atmosphere it will interact with molecules to produce a cascade of secondary particles including protons, electrons, neutrons, and muons, many of which contribute to atmospheric ionisation. A range of GCR detection techniques can therefore be used as indirect measurements of atmospheric ionisation. Some ground-based experiments determine the energy of primary GCRs using Extensive Air Shower (EAS) arrays or Cherenkov radiation, but, as these modern astroparticle physics experiments are usually designed to detect only the highest-energy particles, they are unsuitable for routine monitoring of atmospheric ionisation (e.g. Abraham and the Pierre Auger Observatory Collaboration, 2004; Watson, 2011). The cosmogenic isotope ^{10}Be is produced in the stratosphere and upper troposphere from the bombardment and breakdown (spallation), of N_2 and O_2 nuclei by GCR neutrons; inferring past ^{10}Be generation through assaying its abundance in polar ice sheets provides an indirect (proxy) method for monitoring the long term GCR flux (Lal and Peters, 1967; Beer, 2000). Disadvantages of the ^{10}Be technique are that its production occurs in the stratosphere, and obtaining reliable information from the ^{10}Be record requires accurate representation of environmental processes controlling ^{10}Be production, transport and deposition (Pedro et al., 2011). Surface measurements of GCRs can also be made using muon telescopes, which detect the muon component of the nucleonic cascade. As muons cause most of the GCR ionisation in the lower

* Corresponding author.
  E-mail address: karen.aplin@physics.ox.ac.uk (K.L. Aplin).

troposphere, this approach is useful for ionisation measurement, but the technology is not widely used, as the data has to be corrected for atmospheric variations to obtain the primary GCR flux (e.g. Duldig, 2000).

Extensive regular monitoring of GCRs utilises surface neutron monitors, introduced in the 1950s (Simpson et al., 1953). These devices are sensitive to the neutron component of the nucleonic cascade initiated by the primary GCR particles. As Aplin et al. (2005) pointed out, it is sometimes assumed that neutron monitor data also provides a good estimate of ionisation in the lower troposphere, rather than just at the neutron-producing region of the atmosphere. However, the contribution to atmospheric ionisation from lower-energy particles, which do not necessarily produce neutrons, is also required (e.g. Lindy et al., 2014). This means, for example, that the variability found in situ at the upper level intensity maximum is larger than that in the nucleonic component at the surface, e.g. by a factor of two (Brown, 1959). Models of lower atmosphere ionisation calculate the average vertical profile using standard atmospheric properties (e.g. Usoskin and Kovaltsov, 2006; Mishev, 2013), but, to determine the instantaneous ionisation rates in the real atmosphere, in situ measurements are still required.

A series of in situ soundings of atmospheric ionisation is described here, and compared with both neutron monitor data and modelled profiles. These soundings are evaluated in terms of their use in atmospheric electricity, both in providing parameters for the global atmospheric electric circuit, and for investigating radiative effects of ionisation, such as through effects on clouds.

2. Methodology

Standard meteorological balloon measurement systems, based on radiosonde packages, are routinely used to obtain vertical atmospheric profiles of temperature and relative humidity for weather forecasting purposes. This established infrastructure can also provide an inexpensive platform with which to make vertical measurements of ionisation. A new disposable instrument for meteorological radiosondes has recently been developed (Harrison et al., 2012, 2013a) which is based on two miniature Geiger tubes – a geigersonde – and a set of these instruments has provided the measurements considered here. The geigersonde approach to obtaining ionisation profiles is well-established (e.g. Pickering, 1943; Stozhkov et al., 2009), but, by using a digital interface system with a modern radiosonde (Harrison 2005a; Harrison et al. 2012), the radiosonde's meteorological data can also be retained. Hence, as well as telemetering the total number of events detected since switch-on by the two independent Geiger tubes, the standard meteorological measurements of temperature, pressure, relative humidity, as well as GPS location can be conveyed.

By using the radiosonde's height and position information, the tubes' count rates can provide the vertical ionisation profile. Furthermore, if a range of profiles are obtained that are well separated in time, changes between the launches can be investigated, for example that associated with the solar modulation (Neher, 1967; Sloan et al., 2011). Finally, by releasing the same design of instrument at different launch locations, the variation in ionisation profile with geomagnetic latitude can be determined. In each case, the validity of the ion production profiles can be confirmed through comparison with modelled values and simultaneous surface measurements made using neutron monitors.

The Geiger tubes used in these instruments are Neon–Halogen LND714 beta–gamma detectors, operated at a well-regulated bias voltage of 465 V (Harrison et al., 2013a). This tube has a small detection volume (33 mm length and 5 mm diameter) compared

with typical tubes employed in atmospheric applications, so the count rates from the two tubes are summed to improve the statistics. (A laboratory experiment with an 18 kBq ^{60}Co gamma source confirmed that combining the two count rates also reduced the effect of tube-to-tube variability to better than 2% for the LND714s tested.) The tube's response to gamma radiation from a ^{60}Co source is specified by the manufacturer as 1.5 counts s^{-1} per Roentgen of radioactivity.[1] Using this calibration to determine the charge generated per unit mass of air per count (for which the associated volume can be found under conditions of standard temperature and pressure, STP, defined here as 25 °C and 1000 hPa), and assuming that ions carry a unit elementary charge, the rate of ion production per unit volume of air q_{STP} associated with a count rate X in events min^{-1} can be found as

$$q_{STP} = 2.95X, \tag{1}$$

where q_{STP} is the ionisation rate in number of ions cm^{-3} s^{-1}. As well as providing the bias voltage to operate the tubes, the electronic system records the total number of pulses received from each of the two tubes separately, the operating time, and the interval between the pulses. The pulse interval can provide additional resolution at low count rates, such as in the lower atmosphere, as, if only a few counts occur per minute, the proportional error in the count rate caused by a pulse occurring at the beginning or end of the measuring time can otherwise be appreciable (Harrison et al., 2013a). Measured quantities are transmitted over the standard UHF radio link every 30 s, interleaved with the meteorological data and position information. The data values are processed by calculating the count rates for each tube separately, using a moving 60 s window.

3. Results

3.1. Characterisation of soundings

Geigersonde launches were made from Reading University Atmospheric Observatory (51.442°N, 0.938°W) during 2013 and early 2014 using 200 g helium-filled carrier balloons. These launches were made when an instrument package had been fully constructed and tested, and the meteorological conditions allowed a straightforward single person release; these requirements amounted to a largely random set of releases. This is apparent from the trajectories taken by the geigersondes shown in Fig. 1 showing the different wind directions encountered, which also marks the position where the maximum height was obtained. (Full details of the flights are given in Table 1, including the times of the balloon release. Raw data is available through the corresponding author). Altitudes at which the balloon burst varied between the launches, but most reached at least 20 km.

Fig. 2 shows the vertical profile of measured count rate for soundings reaching at least 25 km, with the count rate obtained using the averaging window technique (Harrison et al., 2013a). In each sounding, the individual data points from the two tubes carried are shown using different plotting symbols, with a cubic spline fitted to smooth the data. All of these soundings show the characteristic form of a small count rate in the lowest few km, increasing sharply from about 5 km to reach a maximum value around 20 km (referred to here as the Regener–Pfotzer,[2] or RP,

---

[1] The Roentgen is no longer a standard unit of radioactivity. It remains useful for determining ion production rates, as it is characterised in terms of the charge released per unit mass (2.658×10^{-4} C kg^{-1}), from which the number of elementary charges produced per unit volume can be calculated.

[2] The important contributions of Erich Regener (1881–1955) whilst working at Stuttgart have been widely neglected (Watson and Carlson, 2014). Regener
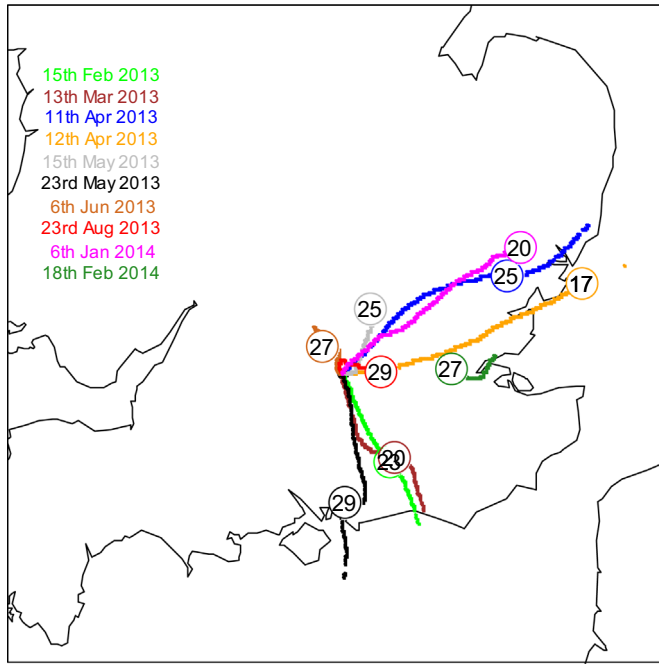
Fig. 1. Trajectories of geigersondes launched from Reading between February 2013 and February 2014. The circle on each trajectory gives the position where the maximum altitude was reached, and the maximum altitude in km. (In most, but not all cases, both ascent and descent data is available.)

Fig. 2. Vertical profiles of count rate obtained from a subset of flights reaching 25 km altitude or greater (a) on 11th April 2013, (b) 23rd May 2013, (c) 6th June 2013 and (d) 23rd August 2013, using counts telemetered every 30 s. The plot symbols are different for the two Geiger tubes carried. An interpolating spline curve has been fitted for smoothing, and to allow estimation of the height of the maximum count rate.

maximum). The fitted spline provides the height of the RP maximum, and the associated time and count rate have been included in Table 1.

Because the count rates are small at low altitudes, the data from both tubes in the geigersondes have been combined to give a mean count rate in vertical layers of 1 km thickness, as shown in Fig. 3a. This is an alternative approach to use of a smoothing spline to reduce the variability, and allows visual comparison between the different flights. Air temperature measurements made during each sounding are provided for comparison in Fig. 3b, to show the associated atmosphere structure. The height at which the air
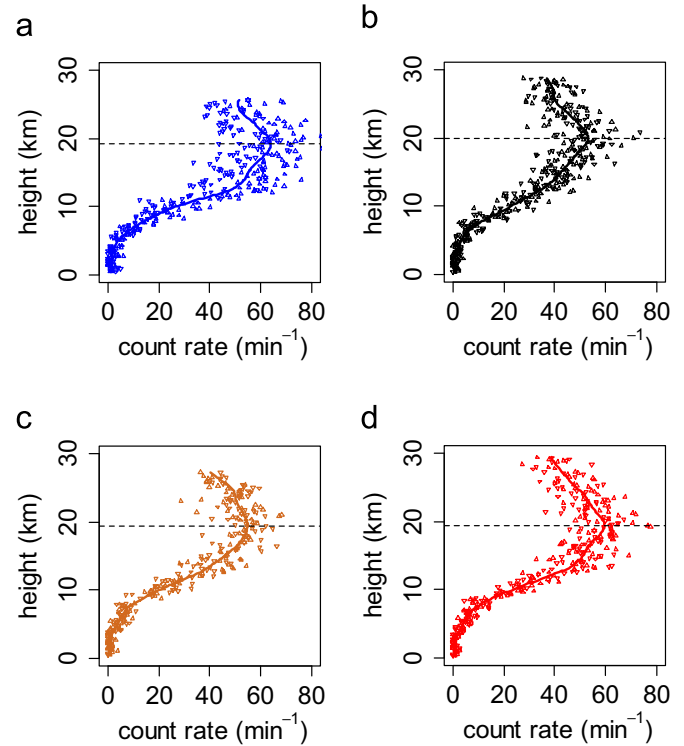
temperature ceases to decrease with height, i. e. the base of the tropopause, varies (as is well known) with the time of year. The increase in temperature above this which marks the base of the stratosphere is broadly consistent with the position of the RP maximum. In comparison, the coarser vertical temperature profile from the US standard atmosphere only approximates each of the real soundings, particularly at the base of the tropopause. For the

Table 1
Characteristics of geigersonde flights.

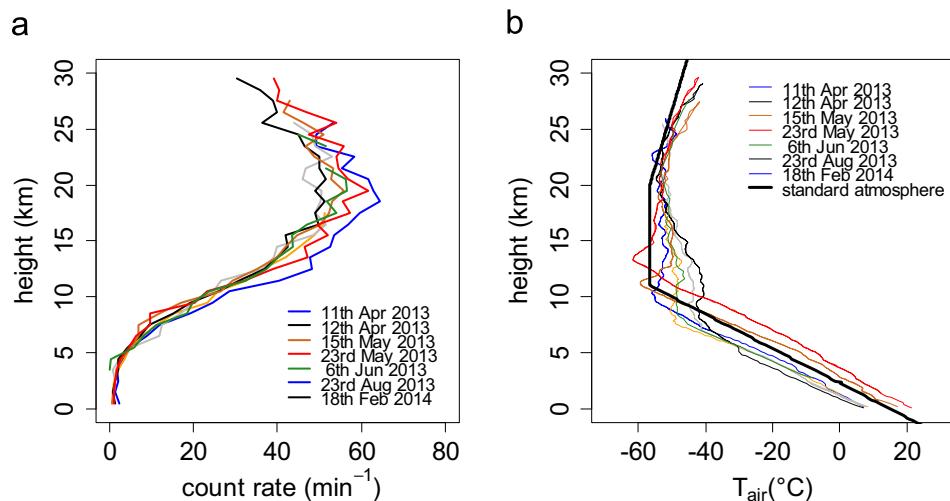| Date	Launch time (UT)	Oulu neutron monitor count rate at launch time	Burst height (km)	Height at which maximum count rate reached (km)	Flight duration to reach maximum count rate (s)	Time at which maximum count rate reached (UT)	Oulu neutron monitor at time of maximum count rate	Meteorological properties (temperature T, pressure P and density ρ) at height of maximum ionisation		
								T (°C)	P (hPa)	ρ (g m^{-3})
6th Feb 2013			16.85							
15th Feb 2013	1400	6301 ± 47	23.93	18.89	3629	1500	6321 ± 50	−63.4	66.8	111
13th Mar 2013	1210	6436 ± 49	20.78							
11th Apr 2013	1219	6304 ± 44	25.97	19.16 (ascent)	4545 (ascent)	1330	6326 ± 49	−53.6	63.9	101
				18.72 (descent)	6350 (descent)	1400	6317 ± 48	−52.7	68.4	108
12th Apr 2013	0831	6288 ± 42	18.18							
15th May 2013	1420	6169 ± 30	25.51	indistinct						
23rd May 2013	1329	6004 ± 46	29.14	19.88	5000	1450	6018 ± 39	−53.1	57.2	90
6th Jun 2013	1230	6111 ± 42	27.72	19.46 (ascent)	4628 (ascent)	1350	6131 ± 50	−54.2	61.0	97
				19.33 (descent)	6718 (descent)	1420	6118 ± 61	−52.8	62.3	99
23rd Aug 2013	0954	6188 ± 40	29.62	19.34	4867	1115	6218 ± 46	−52.7	61.7	98
6th Jan 2014	1720	6284 ± 40	20.36							
18th Feb 2014	1140	6115 ± 39	27.91	19.24 (descent)	6663 (descent)	1330	6089 ± 33	−51.6	63.2	99
Mean values								**−54.2**	**63.1**	**101**
(± 1.96 standard errors)								± 2.6	± 2.4	± 5

Fig. 3. Variations in vertical profiles of (a) count rates from both tubes averaged into vertical layers of thickness 1 km and (b) instantaneous air temperature obtained during the soundings, with US 1976 standard atmosphere over-plotted.
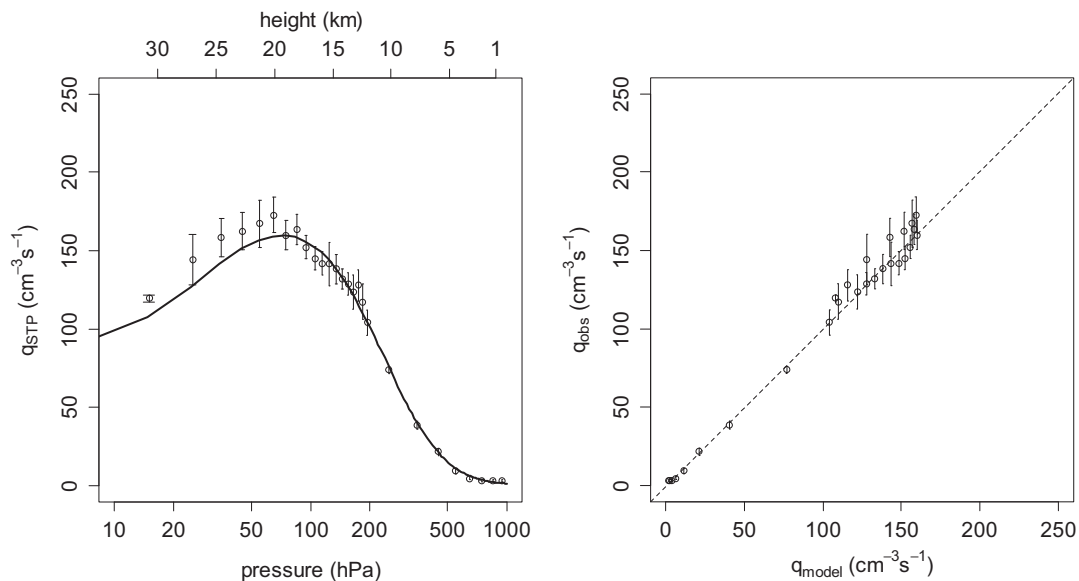

Fig. 4. (Left panel) Comparison of the ion production rate at standard temperature and pressure (q_{STP}) obtained for Reading from the Usoskin–Kovaltsov model (solid lines) and averages of the measured values from all flights (points with error bars). Both the model and measured data are plotted against atmospheric pressure, as determined continuously by the meteorological radiosonde in steps of 10 hPa down to 200 hPa, and then 100 hPa steps. (Right panel) Modelled and observed STP ion production rates q_{model} and q_{obs} plotted against each other with a 1:1 line added. (Error bars in both cases represent 2 standard errors on the mean.)

flight to flight differences in count rates apparent in Fig. 3a, other than the 11th April 2013 flight associated with a solar flare which is discussed elsewhere (Nicoll and Harrison, 2014), the variability cannot be straightforwardly associated with atmospheric structure differences.

3.2. Comparison with ion production rate modelling

Fig. 4 shows the count rates after conversion using Eq. (1) to provide the equivalent ion production rate under standard conditions, q_{stp}. In the left-hand panel of Fig. 4, the q_{stp} values have been

plotted against the air pressure at which they are obtained, as measured by the radiosonde's meteorological sensor. To these values, the predicted ion production rate profile q_{model} for Reading, UK using the model has been added. Below 20 km, there is good agreement between q_{model} and q_{stp}, as also apparent in the right-hand panel. (The exception is in the lowest 1–2 km which is not readily seen in Fig. 4, where, because of surface radioactivity, the measured ionisation rate is up to twice that of the modelled values. This is, however, not a failing in the model, as it only seeks to represent the cosmic ray source of ionisation.) Above 20 km the agreement lessens between the measurements and the Usoskin–Kovaltsov model (worst case error 13%), although this is likely to be influenced by the diminishing amount of data available at the higher altitudes. Previously, for altitudes above the 50 hPa pressure level, Sloan et al. (2011) suggested a discrepancy between the Usoskin–Kovaltsov model and soundings of up to 20%.

(*footnote continued*)
originally identified the region of maximum ionisation, and subsequently described this in a joint paper with his student, Georg Pfotzer (Regener and Pfotzer, 1935). The long-standing use of the description "Pfotzer maximum" is therefore incomplete and historically inadequate.
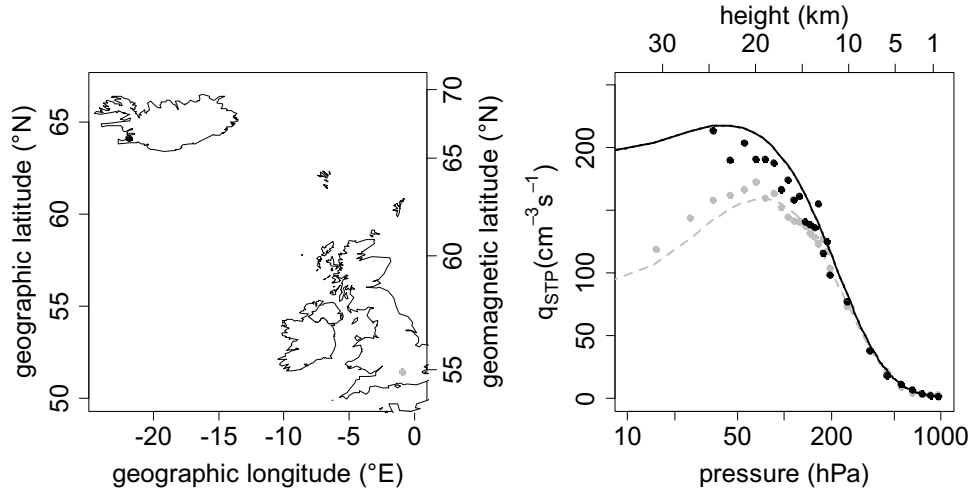
Fig. 5. (Left) Positions of the geigersonde launch sites at Reykjavik, Iceland (64.1275°N, −21.9028°E, black point) and Reading, UK (51.442°N, −0.938°E, grey point), with the geomagnetic latitude also shown on the right-hand axis. (Geomagnetic latitude calculated at −10°E for 2013, using the International Geomagnetic Reference Field, IGRF-11.) (Right) Mean values of measured ion production rate q_{STP} against atmospheric pressure using the ascents from Reading (grey points), and Reykjavik (black points), with calculated q_{STP} from the Usoskin–Kovaltsov model for Reading and Reykjavik also shown (grey and black lines respectively).

The Usoskin–Kovaltsov model is able to predict the ionisation profile at any geomagnetic latitude. Three further soundings were made during 22nd and 23rd August 2013 in Reykjavik, Iceland, which is about 10° further north in geomagnetic latitude than Reading (see left panel of Fig. 5.) The average q_{stp} found from these three flights is shown in the right panel of Fig. 5, with the q_{model} values added as a line, and the equivalent values from Reading are also shown. There is, again, good agreement at altitudes below the 50 hPa pressure level, with the agreement diminishing as altitude increases. Notably, the RP maximum is much less distinct in q_{model} for the higher latitude of Reykjavik compared with the model results for Reading, which is supported by both the measured q_{stp} values, and previous observations at more northerly latitudes (e.g. Neher, 1967). However, the generic form of the ionisation profile, with a slow increase in the lower troposphere to a maximum in the lower stratosphere, is still apparent.

By combining the data obtained from all the flights from Reading where the RP maximum could be identified (Table 1), the mean pressure at the maximum was determined as (63.1 ± 2.4) hPa and the air temperature (-54.2 ± 2.6) °C, with an associated air density (0.101 ± 0.005) kg m^{-3}, where the uncertainties represent 1.96 standard errors in each case. The (pressure) position of the maximum ionisation rate in the

Usoskin–Kovaltsov calculations for Reading is at 73.3 hPa, which, under the standard atmosphere assumption, corresponds to -56.5 °C and an air density of 0.116 kg m^{-3}.

3.3. Temporal variations

During the period of the launches listed in Table 1, variations in the galactic cosmic ray flux occurred, associated with the weak solar maximum conditions. Fig. 6 shows the daily time series of count rate at the Oulu neutron monitor (NM) with the dates of the launches marked. It is evident that the cosmic ray environment differed markedly between some of the launches. Variations in the surface NM count rates are expected to originate in the nucleonic generation rate at the RP maximum. Fig. 7 plots the count rate obtained when the balloon soundings are at the RP maximum against the NM count rate measured at the same time, as summarised in Table 1. The neutron monitor count rate and the RP count rates are positively correlated, and, if a linear fit is made between the two parameters assuming the least-squares criterion, the proportional changes in the RP count rate are (3.0 ± 1.2) greater than those in the NM, which is not inconsistent with the enhancement of 2.2 reported by Brown (1959).
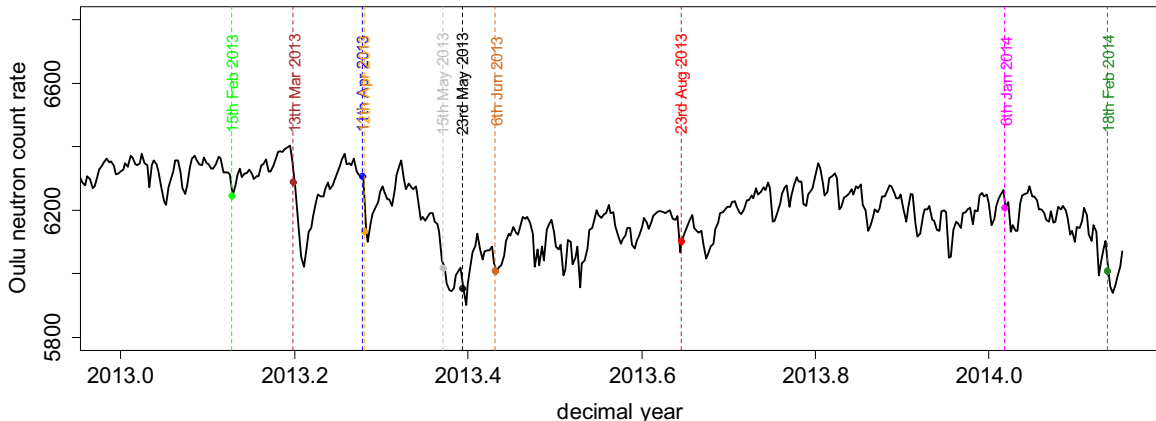

Fig. 6. Variation in the Oulu neutron monitor count rate measured during the Reading Geigersonde measurements. (The flight dates are marked.)
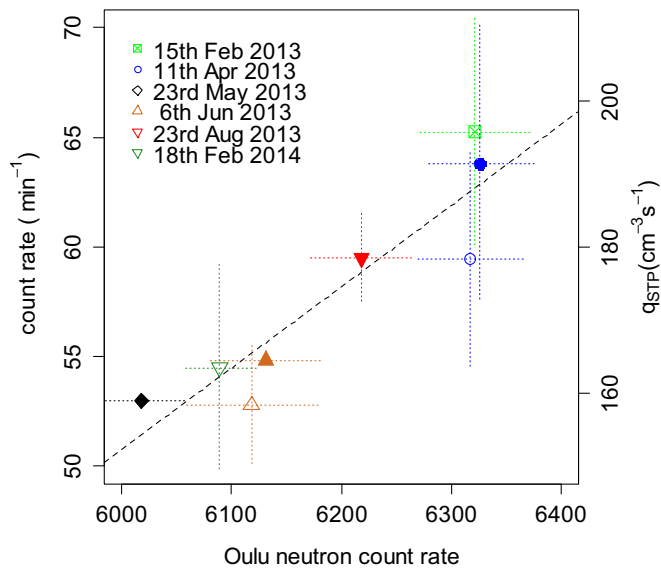
Fig. 7. Comparison between count rates obtained at the Regener–Pfotzer maximum (as identified using the spline method), and surface neutron monitor data from Oulu. Error bars in the geigersonde data represent the spread of the two tubes, and the error bars in the neutron monitor two standard errors during the 30 min period centred on the time when the Regener–Pfotzer maximum was reached. (Solid points represent ascent data, hollow points represent descent data.)

3.4. Vertical profile information

As well as comparing the NM data with the count rates at the RP maximum, the count rates at all other available heights (vertical resolution 1 km as for Fig. 3) across the flights can be compared with the NM values at the same times. Fig. 8a shows the correlation between the geigersonde count rates and the associated Oulu NM count rate at the launch time. The number of values available at each height depends on the reliability of the telemetry and the burst height, which is given in Fig. 8b. Statistically significant correlations in Fig. 8a and c are identified with points. Fig. 8c shows the correlation between the geigersonde count rate at the RP maximum (for those flights when this could be identified) with the geigersonde count rates at other altitudes. The region of stronger significant correlations lies between about 8 km and 22 km, indicating that there is little information on the lower atmosphere ionisation rate available from the RP maximum ionisation region.

4. Discussion

Neutron monitor (NM) data has been widely used in the search for correlations between cosmic rays and atmospheric processes, notably that between galactic cosmic rays and satellite-derived observation of low cloud amount. The usefulness of neutron monitor data in providing information on the actual atmospheric
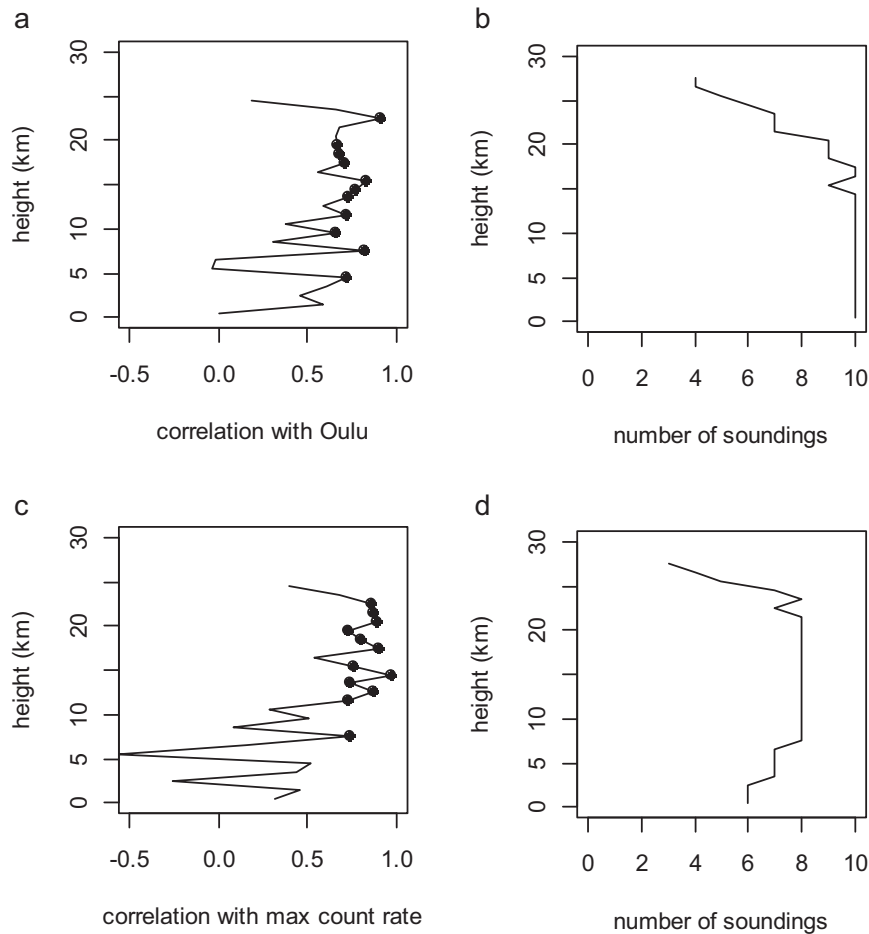

Fig. 8. Correlation between count rates averaged into 1 km layers with, (a) the Oulu surface neutron monitor count rate at the launch time for ascents only, and, (c) the count rate at the Regener–Pfotzer maximum (where reached), for ascents and descents. (b) and (d) show the associated number of values available at each height with which to calculate the correlation. (Points have been added to (a) and (c) to identify correlations which are statistically significant at 95%.)

ionisation at cloud heights is therefore an important consideration (e.g. Harrison and Carslaw, 2003). From Fig. 8, it is apparent that the majority of stronger and significant correlations are at the higher (10–20 km) altitudes, i. e. that the NM data are most useful for estimating the ionisation rate between 10 km and 20 km. Below 10 km, the possibility that the correlations obtained between the launch time NM count rate and the in situ count rate occur by chance cannot be discounted. Whilst this may be partially due to the small count rates at the lower levels, or indeed the contribution of surface radioactivity, Bazilevskaya et al. (2008) also show that the correlation between in situ measurements and NM data decreases substantially below 1 km. Hence it is unlikely that short-term variations in atmospheric ionisation are well predicted by NM data, for the typical timescales associated with balloon flights of a few hours. For monthly timescales, a closer agreement is apparent in the lower atmosphere, such as at 700 hPa (e.g. Usoskin and Kovaltsov, 2006). Consequently the rapid onset of a Forbush decrease which is apparent in NM data may not provide a good representation of the actual atmospheric short-term ionisation changes at cloud levels. This may, in part, provide an explanation for the differences found in the response of clouds to monthly and Forbush changes (Calogovic et al., 2010).

In terms of the atmospheric electricity changes arising from variations in atmospheric conductivity, the NM data may also be far from ideal for indicating transient or short-term changes. This is because the vertical profile of atmospheric conductivity has to be integrated to obtain the resistance of a unit area column of atmosphere between the surface and the ionosphere, which determines the local current flow. The majority of the integrated columnar resistance arises from the poorer conductivity in the lower atmosphere, with approximately 70% of the columnar resistance contributed by the lowest 3 km (Harrison and Bennett, 2007). In this region there will be variable contributions from surface radioactivity, and, as Fig. 8 shows, the NM data provides only a poor estimate of the GCR ionisation. At the upper levels from 10 to 20 km, where the NM data does provide a much better estimate of the total ionisation, only about 10% of the columnar resistance remains to be affected by GCR ionisation. Thus the NM data cannot be expected to provide a good estimate of the total columnar resistance in general, at least on the typical timescales of the balloon flights considered, for which improved parameterisations are needed. Instead, the columnar resistance can be found by using integrated in situ conductivity profiles, or through the use of simultaneous ionospheric potential and surface current density measurements (e.g. Harrison, 2005b). For longer period analyses, in which some of the random variability in the lower atmosphere can be expected to be reduced by averaging, the NM data can still provide an indication of the lower atmosphere ionisation changes (e.g. Harrison et al. 2013b).

Finally, the properties of the atmosphere assumed by using the US standard atmosphere only approximate the local atmospheric properties found in one particular season, as apparent from Fig. 3. As discussed in Aplin et al. (2005), reanalysis data from meteorological soundings is now widely available at better than daily resolution which will provide better representation of the atmosphere for modelling purposes than the standard atmosphere assumption. Of course, a particular advantage of using meteorological radiosondes for ionisation measurements is that temperature, pressure, height and location are measured simultaneously with the ionisation rate.

Acknowledgements

References

Abraham, J., the Pierre Auger Observatory Collaboration, 2004. Properties and performance of the prototype instrument for the Pierre Auger Observatory. Nucl. Instrum. Methods. Phys. Res. Sect. A: Accel. Spectrom. Detect. Assoc. Equip. 523 (1), 50–95.

Aplin, K.L., Harrison, R.G., Bennett, A.J., 2005. Effect of the troposphere on surface neutron counter measurements. Adv. Space Res. 35, 1484–1491.

Aplin, K.L., Lockwood, M., 2013. Cosmic ray modulation of infra-red radiation in the atmosphere. Environ. Res. Lett. 8, 015026.

Beer, J., 2000. Long-term indirect indices of solar variability. Space Sci. Rev. 94 (1–2), 53–66.

Bazilevskaya, G.A., Usoskin, I.G., Flückiger, E.O., Harrison, R.G., Desorgher, L., Bütikofer, R., Kovaltsov, G.A., 2008. Cosmic ray induced ion production in the atmosphere. Space Sci. Rev. 137 (1–4), 149–173.

Brown, R.R., 1959. Excess radiation at the Pfotzer maximum during geophysical disturbances. J. Geophys. Res. 64 (3), 323–329.

Calogovic, J., Albert, C., Arnold, F., Beer, J., Desorgher, L., Flueckiger, E.O., 2010. Sudden cosmic ray decreases: no change of global cloud cover. Geophys. Res. Lett. 37, L03802. http://dx.doi.org/10.1029/2009GL041327.

Duldig, M., 2000. Muon observations. Space Sci. Rev. 93 (1–2), 207–226.

Harrison, R.G., 2005a. Meteorological radiosonde interface for atmospheric ion production rate measurements. Rev. Sci. Instrum. 76, 126111.

Harrison, R.G., 2005b. Columnar resistance changes in urban air. J. Atmos. Sol.-Terr. Phys. 67 (8–9), 763–773.

Harrison, R.G., Bennett, A.J., 2007. Cosmic ray and air conductivity profiles retrieved from early twentieth century balloon soundings of the lower troposphere. J. Atmos. Sol.-Terr. Phys. 69 (4–5), 515–527. http://dx.doi.org/10.1016/j.jastp.2006.09.008.

Harrison, R.G., Carslaw, K.S., 2003. Ion-aerosol-cloud processes in the lower atmosphere. Rev. Geophys. 41 (3), 1012.

Harrison, R.G., Nicoll, K.A., Lomas,, A.G., 2012. Programmable data acquisition system for research measurements from meteorological radiosondes. Rev. Sci. Instrum. 83, Art no. 036106.

Harrison, R.G., Nicoll, K.A., Lomas, A.G., 2013a. Geiger tube coincidence counter for lower atmosphere radiosonde measurements. Rev. Sci. Instrum. 84, 076103.

Harrison, R.G., Nicoll, K.A., McWilliams, K.A., 2013b. Space weather driven changes in lower atmosphere phenomena. J. Atmos. Sol.-Terr. Phys. 98, 22–30.

Kirkby, J., Curtius, J., Almeida, J., Dunne, E., et al., 2011. Role of sulphuric acid, ammonia and galactic cosmic rays in atmospheric aerosol nucleation. Nature 476, 429–433. http://dx.doi.org/10.1038/nature10343.

Lal, D., Peters, B., 1967. Cosmic ray produced radioactivity on the Earth. In: Flugge, S. (Ed.), Handbuch der Physik, 46. Springer, Berlin, Heidelberg, pp. 551–612.

Lindy N.C., Benton E.R., Ruse A.N., and Beasley W., (2014), The cosmic-ray extensive air shower environment of thunderstorms. In: Proceedings of the International Conference on Atmospheric Electricity, Norman, Oklahoma, June 16th–20th, 2014, ⟨http://www.nssl.noaa.gov/users/mansell/icae2014/preprints/Lindy_152.pdf⟩.

Mishev, A., 2013. Short- and medium-term induced ionization in the earth atmosphere by galactic and solar cosmic rays. Int. J. Atmos. Sci. 2013, 184508. http://dx.doi.org/10.1155/2013/184508 (9 pp.).

Neher, H.V., 1967. Cosmic ray particles that changed from 1954 to 1958 to 1965. J. Geophys. Res. 72 (5), 1527–1539.

Nicoll, K.A., Harrison, R.G., 2010. Experimental determination of layer cloud edge charging from cosmic ray ionisation. Geophys. Res. Lett. 37, 13802.

Nicoll, K.A., Harrison, R.G., 2014. Detection of lower tropospheric responses to solar energetic particles at mid latitudes. Phys. Rev. Lett. 112, 225001–225005.

Pedro, J.B., Smith, A.M., Simon, K.J., van Ommen, T.D., Curran, M.A.J., 2011. High-resolution records of the beryllium-10 solar activity proxy in ice from Law Dome, East Antarctica: measurement, reproducibility and principal trends. Clim. Past 7, 707–721.

Pickering, W.H., 1943. An improved cosmic-ray radiosonde. Rev. Sci. Instrum. 14 (6), 171–173.

Regener, E., Pfotzer, G., 1935. Vertical intensity of cosmic rays by threefold coincidences in the stratosphere. Nature 136, 718–719.

Rycroft, M.J., Israelsson, S., Price, C., 2000. The global atmospheric electric circuit, solar activity and climate change. J. Atmos. Sol.-Terr. Phys. 62 (17), 1563–1576.

Simpson, J.A., Fonger, W., Treiman, S.B., 1953. Cosmic radiation intensity-time variations and their origin. I. Neutron intensity variation method and meteorological factors. Phys. Rev. 90, 934–950.

Sloan, T., Bazilevskaya, G.A., Makhmutov, V.S., Stozhkov, Y.I., Svirzhevskaya, A.K., Svirzhevsky,, N.S., 2011. Ionization in the atmosphere, comparison between

measurements and simulations. Astrophys. Space Sci. Trans. 7, 29–33. http://dx.doi.org/10.5194/astra-7-29-2011.

Stozhkov, Y.I., Svirzhevsky, N.S., Bazilevskaya, G.A., Kvashnin, A.N., Makhmutov, V.S., Svirzhevskaya, A.K., 2009. Long-term (50 years) measurements of cosmic ray fluxes in the atmosphere. Adv. Space Res. 44, 1124–1137.

Usoskin, I.G., Kovaltsov, G.A., 2006. Cosmic ray induced ionization in the atmosphere: Full modeling and practical applications. J. Geophys. Res. Atmos. 111, D21. http://dx.doi.org/10.1029/2006JD007150.

Watson, A.A., 2011, The discovery of Cherenkov radiation and its use in the detection of extensive air showers. In: Proceedings of CRIS2010: Cosmic Ray International Seminar on'100 years of Cosmic Rays: from Pioneering Experiments to Physics in Space'.

Watson, A.A., Carlson, P., 2014. Erich Regener – a forgotten cosmic-ray pioneer. Hist. Geo Space Sci. (accepted for publication).